Modeling the evaporation from a thin liquid surface beneath a turbulent boundary layer

Thomas Vik og Bjørn Anders Pettersson Reif

Norwegian Defence Research Establishment (FFI)

15 October 2010

FFI-rapport 2010/00254

114902

P: 978-82-464-1820-9
E: 978-82-464-1821-6

Keywords

Fordampning

Turbulent strømning

Turbulent grensesjikt

Approved by

Monica Endregard	Project Manager
Jan Ivar Botnan	Director

English summary

The release and dispersion of toxic chemicals can cause a threat to military personnel and the population at large. In order to develop and implement appropriate protective capabilities and plan mitigating measures, modeling, simulation and assessments of hypothetical scenarios and historical incidents is a valuable and widely used methodology. This requires reliable CBRN modeling and simulation capabilities to model how toxic chemicals are released and dispersed in air.

A physical and mathematical model of an event involving the dispersion of chemicals can roughly be divided into three parts: source modeling, transport modeling and effect modeling. This study focuses on source modeling.

As part of the recent NATO-study SAS-061, research groups in the U.S., The Netherlands and FFI assessed the same scenario which involved release of the chemical warfare agent (CWA) sarin. The groups used an evaporation rate for sarin which varied by a factor of 10. This leads to correspondingly large variations of the calculations of the consequences and the extent of damage. This introduces an unacceptable uncertainty in consequence assessments and clearly demonstrates the need to improve our fundamental knowledge of evaporation processes.

The current work is a continuation of work done previously at FFI. Odd Busmundrud developed a model for evaporation from surfaces and droplets. His model is in essence based on molecular diffusion through an assumed wind-free diffusion layer above the surface, and only indirectly takes account for fluid dynamical aspects of the evaporation process. The present study considers the evaporation of a non-buoyant contaminant from a thin liquid surface beneath a turbulent boundary layer. The analysis is based on near-surface asymptotics of turbulence velocity and scalar fluctuations. The objective of the study is to derive and verify an algebraic evaporation model sensitized to boundary layer turbulence. The dependence on the friction velocity is shown to be naturally included in the analysis and the model does not depend on any *a priori* assumption of the existence of an equilibrium logarithmic boundary layer region. The near-surface asymptotics are fairly universal and thus valid for a wide range of external flow conditions. The model is validated using recent experimental wind tunnel data. This work will be continued by including the model in CFD software.

It is crucial to have access to good quality experimental data. In order to isolate the dependence on different aspects on the evaporation process (thermal effects, turbulence, the size of the liquid surface etc), measurements where the different parameters are systematically varied are necessary. It would be of great value to perform such measurements ourselves. Especially for toxic chemicals and chemical warfare agents (CWA) such data are hard to get.

Sammendrag

Utslipp og spredning av giftige kjemikalier kan utgjøre en trussel mot militært personell og befolkningen i allmennhet. Modellering, simulering og analyse av hypotetiske scenarier og historiske hendelser en svært verdifull og mye brukt metode for å utvikle og implementere passende beskyttelseskapabiliteter og planlegge beskyttelses- og mottiltak. Dette krever at prosesser der giftige kjemikalier slippes ut og spres i luft kan modelleres og simuleres på en troverdig måte.

En fysisk og matematisk modellering av en spredningshendelse kan grovt sett deles inn i tre deler: kildemodellering, transportmodellering og effektmodellering. Denne studien tar fokuserer på kildemodellering.

I en NATO-studie nylig gjennomført, SAS-061, analyserte forskningsgrupper i USA, Nederland og FFI hver for seg et scenario som involverte spredning av det kjemiske trusselstoffet sarin. De ulike gruppene benyttet fordampingsrater som varierte med en faktor 10. Dette medfører tilsvarende store variasjoner i beregninger av konsekvenser og skadeomfang. Dette gir en uakseptabel usikkerhet i konsekvensvurderingene og demonstrerer videre nødvendigheten av å forbedre vår fundamentale kunnskap om fordamingsprossesser.

Dette arbeidet er en videreføring av tidligere arbeid på FFI. Odd Busmundrud utviklet en modell for fordamping fra dråper og overflater. Hans modell baserer seg i hovedsak på molekylær diffusjon gjennom et tenkt stillestående luftlag over overflaten, og tar kun indirekte hensyn til strømningstekniske effekter på fordampningsprosessen. Studien som presenteres i denne rapporten tar for seg fordampning av en nøytral kontaminant fra en tynn væskeoverflate under et turbulent grensesjikt. Analysen er basert på det turbulente hastighetsfeltet og fluktuasjoner nær en overflate. Målet med studien er å utvikle og verifisere en algebraisk fordampningsmodell som er følsom for grensesjiktsturbulens. Avhengigheten av friksjonshastigheten vises å være naturlig inkludert i analysen, og modellen avhenger ikke av noen *a priori* antagelser om eksistensen av en logaritmisk grensesjiktetsregion i likevekt. Det turbulente hastighetsfeltet og fluktuasjonene nær vegg er forholdsvis universelle og dermed gyldig for et stort spekter av eksterne strømningsforhold. Modellen er validert ved bruk av eksperimentelle data fra vindtunneleksperimenter. Arbeidet vil ble videreført ved å inkludere modellen i CFD-software.

Det er svært viktig å ha tilgang til gode eksperimentelle data. For å undersøke påvirkningen av ulike aspekter på fordampningen (termiske effekter, turbulens, væskeoverflatens størrelse osv), er det nødvendig med gode målinger der de ulike parametrene varieres på en systematisk måte. Det vil være av stor nytte å selv kunne foreta slike målinger. Spesielt for skarpe stridsmidler er det vanskelig å få tak i gode eksperimentelle data.

Contents

1	**Introduction**	**7**
2	**Background**	**8**
3	**Mathematical modeling**	**10**
3.1	The boundary layer limit	11
3.1.1	The near-surface limit	12
3.2	Algebraic evaporation models	14
3.2.1	Model for the total evaporation time	15
3.3	Odd Busmundrud's model	15
4	**Results**	**16**
5	**Concluding remarks**	**18**
	Bibliography	**21**

1 Introduction

Release and aerial dispersion of toxic chemicals may pose a threat to military personnel and the population in general. In order to develop and implement appropriate protective capabilities and plan mitigating measures, modelling, simulation and assessments of hypothetical scenarios and historical incidents is a valuable and widely used methodology. This requires reliable CBRN modelling and simulation capabilities to model how toxic chemicals are released and dispersed in air.

A complete model for an event involving toxic chemical can roughly be divided into three parts: source modeling, transport modeling and effect modeling[1]. The present study concerns source modeling.

As part of the recent NATO-study SAS-061, research groups in the U.S., The Netherlands and FFI assessed the same scenario which involved release of the chemical warfare agent (CWA) sarin [2]. The groups used an evaporation rate for sarin which varied by a factor of 10. This huge variation demonstrates the uncertainty about the true evaporation rate at various temperatures and introduces an unacceptable uncertainty in consequence assessments. It clearly demonstrates the need to improve our fundamental knowledge of evaporation processes.

The objective of the present work is to develop an improved mathematical model for evaporation of toxic chemicals from pools and droplets in air, including aerosols. The model will subsequently be implemented and used in dispersion modelling on a local scale in Computational Fluid Dynamics (CFD) software and operational dispersion model and consequence assessment software. The focus of this study is evaporation of toxic chemicals which are liquids at ambient conditions with boiling points above 100°C, such as CWA and CWA simulants.

The work is divided in two main parts

- Development of an analytical mathematical model for evaporation basically from first principles
- Comparison of the evaporation model with experimental measurements

Chapter 2 gives an overview of the field, while the theory for the current models are presented in chapter 3. Comparison with published experimental results are given in chapter 4, and chapter 5 gives some concluding remarks.

2 Background

Current approaches to predict the evaporation rates from liquid surfaces fall into two categories: simplified algebraic formulas and Computational Fluid Dynamics (CFD). The latter is based on numerical solutions of the fundamental equations governing conservation of mass, momentum, and energy, and is particularly well suited to model contaminant dispersion and transport on local scales (1-2 km^2). Oftentimes, the scale separation between the scale of the source (the liquid surface in this case; usually $\ll$ 1 m^2) and the scale over which contaminant transport is being modeled is very large, making this multiscale problem computationally very demanding and time consuming to solve; it becomes impractical to computationally resolve both the source and to compute the subsequent contaminant transport other than over very short distances. It is therefore beneficial to combine a simple algebraic formula to model the evaporation from the small-scale source with the CFD approach to model the subsequent vapor transport.

The majority of existing algebraic evaporation models have been developed for ambient conditions in still air, see e.g. the review by Winter et. al. [3]. The evaporation of deposited liquid is in most situations, however, affected by an external air stream which under most practical circumstances are fully turbulent. This affects the rate of evaporation as the ability to mix both momentum and contaminant fields are significantly enhanced; firstly, turbulent advection increases the shear forces on the liquid surface due to vertical momentum transport within the boundary layer, and secondly, the passing airstream increases the rate of vapor transport away from the liquid surface.

There is a large body of literature addressing the issue of free-surface evaporation. Sutton [4] considered the downwind vapor transport from a two-dimensional strip of a liquid surface on the ground. An analytical model was derived by assuming a constant velocity field in combination with a power-law variation of the vertical (wall-normal) velocity component. A simple turbulent diffusivity model was used to account for turbulent mixing in the boundary layer. Pasquill [5] argued that the thermal diffusivity should replace the kinematical viscosity of air used in Sutton's analysis. Pasquill's view is, however, not consistent with current concepts of the role of molecular viscosity and diffusivity in turbulent transport; molecular viscosity cannot be neglected since it is directly associated with the rate of turbulence energy dissipation. Brighton [6] realized that and followed the route of Sutton, but introduced molecular viscosity in the analysis based on the argument that the eddy-diffusivity should vary linearly with the distance y to the liquid surface, as put fourth by Hunt and Weber [7]. This approximation is valid in the logarithmic layer of an equilibrium boundary layer. The extent of this region depends on the wall-shear stress, and it starts outside the near-surface layer in which the dominating evaporation processes takes place.

Dooley et al. [8] presented new data on the convective evaporation of sessile droplets from wind tunnel experiments. The novelty of these experiments, which make them particularly valuable here, are the carefully measured time averaged wall-shear stresses. The wall shear stresses defines the so-called friction velocity which is the characteristic velocity scale for turbulent fluctuations near solid boundaries, and thus also the relevant velocity scale with regard to the influence of turbulence on the rate of evaporation. Navaz et al. [9] used these data to systematically validate a semi-

analytical model for convective evaporation. Good agreement with measurements were obtained. While Navaz et al. [9] in fact recognized the role of the wall shear stress on convective evaporation, the postulated dependence of the friction velocity was largely ad hoc.

There has been some work on evaporation modeling at FFI previously. Odd Busmundrud developed a model for the evaporation from surfaces and droplets [10]. In this model, evaporated mass is transported by molecular diffusion from the surface through a wind-free layer above the surface; outside this diffusion layer all the evaporated mass is assumed to be carried away by the air stream. The thickness of the still diffusion layer as function of the free stream air speed is calculated by an empirical expression. This model gives a constant evaporation rate in time. Fluid dynamical effects is indirectly taken into account by the empirical relationship between the diffusion layer and the free-stream air speed.

The present study considers the evaporation of a non-buoyant contaminant from a thin liquid surface beneath a turbulent boundary layer. The objective of the study is to derive and verify an algebraic evaporation model sensitized to boundary layer turbulence. Recent data from evaporation experiments conducted in a controlled wind-tunnel environment [8, 9] will be used to verify the model and its sensitivity to frictional forces on the liquid-air interface.

3 Mathematical modeling

Consider turbulent flow of an incompressible fluid passing over an impermeable solid boundary. The components of the instantaneous velocity and concentration fields can be decomposed as $\tilde{u}_i(\mathbf{x},t) = U_i(\mathbf{x},t) + u_i(\mathbf{x},t)$ and $\tilde{c}(\mathbf{x},t) = C(\mathbf{x},t) + c(\mathbf{x},t)$, respectively, where $U_i = \langle \tilde{u}_i \rangle$ and $C = \langle \tilde{c} \rangle$ denote ensemble averaged quantities and u_i and c are the corresponding fluctuating parts.

In this section we derive a model for the rate of evaporation of liquid chemicals influenced by boundary layer turbulence. The derivation starts from the equation governing the transport of the ensemble averaged concentration field derivable from first principles. It is also assumed that the vapor does not significantly change the volume averaged molecular weight of the air. The latter implies that the vapor can be treated as a *passive* scalar field which simplifies the derivation. The terminology 'passive' alludes to the notion that the contaminant does not affect the velocity and pressure fields. Desoutter et al. [11] studied the impact of density differences between vapor and air on both the dynamics of the near-wall turbulence structures and the evaporation process, and showed that it is significant. These considerations are as already alluded to outside the scope of this study, but a further refinement of the present approach should preferably take these effects into account.

The transport of an instantaneous passive scalar $\tilde{c}(\mathbf{x},t)$ is governed by the advection-diffusion equation

$$\frac{\partial \tilde{c}(\mathbf{x},t)}{\partial t} + \tilde{u}_k(\mathbf{x},t)\frac{\partial \tilde{c}(\mathbf{x},t)}{\partial x_k} = \alpha \frac{\partial^2 \tilde{c}(\mathbf{x},t)}{\partial x_k \partial x_k} + \tilde{\mathcal{S}}(\mathbf{x},t). \tag{3.1}$$

The second term on the left hand side signifies the effect of turbulence which dominates the mixing and transport of $\tilde{c}(\mathbf{x},t)$ as compared to molecular diffusion. The latter process is represented by the term on the right hand side where α is the molecular diffusivity of the contaminant. In order to account for the presence of a liquid pool or droplet, a source term, $\mathcal{S}$, has been added. As long as the liquid pool remains finite it will act as a source for the vapor.

The corresponding transport equation for the ensemble contaminant field can be derived by decomposing the scalar and velocity fields into ensemble averaged and fluctuating parts. The result reads

$$\frac{\partial C(\mathbf{x},t)}{\partial t} + U_k(\mathbf{x},t)\frac{\partial C(\mathbf{x},t)}{\partial x_k} = \alpha \frac{\partial^2 C(\mathbf{x},t)}{\partial x_k \partial x_k} - \frac{\partial \langle c u_k \rangle}{\partial x_k} + \mathcal{S}(\mathbf{x},t) \tag{3.2}$$

where $\langle c u_k \rangle$ denotes the turbulent scalar flux in the x_k direction. This term represents the ensemble averaged effect of turbulent advection on the mean contaminant field and is *a priori* unknown. The passive scalar flux is commonly modeled through a simple gradient diffusion assumption,

$$\langle c u_k \rangle = -\frac{\nu_T}{Pr_T}\frac{\partial C}{\partial x_k}. \tag{3.3}$$

Here, Pr_T is the so-called turbulent Prandtl number, which is not a material property but a property of the flow field. In its most simplistic form it takes a constant value; for boundary layer flows $Pr_T \approx 0.9$ is often used. Pr_T will be taken as a constant here. The eddy viscosity, ν_T, is here assumed to be related to the second moments of velocity fluctuations through the linear constitutive relation

$$\langle u_i u_j \rangle = \frac{\delta_{ik}}{3}\langle u_j u_j \rangle - \frac{\nu_T}{2}\left(\frac{\partial U_i}{\partial x_j} + \frac{\partial U_j}{\partial x_i}\right) \tag{3.4}$$

that appears in the equation governing the conservation of mean momentum. Although ν_T has the same dimensions as the kinematic viscosity of the fluid, e.g. m^2/s, it is not a material property, but depends on the turbulent flow field itself.

The ensemble averaged source term ($\mathcal{S}(\mathbf{x},t)$) in (3.2) is modeled assuming equilibrium in the sense that $\mathcal{S} \propto -\partial C(\mathbf{x},t)/\partial t$. This term is *a priori* unknown since it implicitly depends on the rate of evaporation. The following model is proposed:

$$\mathcal{S}(\mathbf{x},t) = \left(1-\delta_m^{-1}\right)\frac{\partial C(\mathbf{x},t)}{\partial t}. \tag{3.5}$$

where

$$\delta_m = \frac{v_{vapor}\int\int\int C(\mathbf{x},t)dtdA}{m_0} \tag{3.6}$$

is the ratio of the mass of vapor to the initial liquid mass. The dimensionless parameter $(1-\delta_m^{-1})$ in (3.5) ensures that $\mathcal{S} \to 0$ as all liquid has evaporated. In (3.6), m_0 and v_{vapor} denote the initial liquid mass and vertical vapor velocity respectively.

3.1 The boundary layer limit

Flow in the immediate vicinity of impermeable boundaries can to a good approximation be treated as parallel, i.e. $U_k = (U(z),\ 0,\ 0)$ (if we e.g. choose z as the wall-normal coordinate axes). Although only one component of the mean velocity is nonzero (the streamwise velocity component, $U_1 = U$), the turbulent fluctuations are present in all three directions. The only relevant coordinate direction in this case is $x_3 = z$ (corresponding to the wall-normal direction). This implies that all statistical terms only depends on z, i.e. $U(z)$ and $\langle cu_k\rangle(z)$ only.

It should be noted that boundary layer flows in general are not exactly parallel; the velocity field depends on both the streamwise (x) and wall-normal (z) directions. The wall-normal mean velocity component is therefore not zero, but $W \ll U$. The streamwise development of the boundary layer is significantly slower than the variation of the flow in the wall-normal direction. Since we here primarily is interested in relatively small liquid pools, we can to a good approximation neglect the dependence on x and thus assume $W \approx 0$.

Equation (3.2) can thus be written as

$$\frac{\partial C(z,t)}{\partial t} = \alpha\frac{\partial^2 C(z,t)}{\partial z^2} - \frac{\partial\langle cw\rangle}{\partial z} + \mathcal{S} = (\alpha+\alpha_T)\frac{\partial^2 C(z,t)}{\partial z^2} + \mathcal{S}(\mathbf{x},t). \tag{3.7}$$

The last equality is obtained by using (3.3) where the turbulent diffusivity $\alpha_T \sim \nu_T$. It can be concluded that only the wall-normal scalar flux ($\langle cw\rangle$) is relevant to model the transport of $C(z,t)$. It should also be noted that the transport of the ensemble averaged concentration is independent of the scalar variance $\langle c(\mathbf{x},t)^2\rangle$; this property originates from the linearity of (3.1).

3.1.1 The near-surface limit

By conducting a Taylor series expansion in the asymptotic limit as an impermeable boundary is approached (i.e. small z), the fluctuating concentration and velocity components can be written as

$$\begin{aligned} u &= a_0 + a_1 z + a_2 z^2 + O(z^3) \\ v &= b_0 + b_1 z + b_2 z^2 + O(z^3) \\ w &= d_0 + d_1 z + d_2 z^2 + O(z^3) \\ c &= e_0 + e_1 z + e_2 z^2 + O(z^3) \end{aligned}$$

The near-surface limiting behavior of the fluctuating velocity components are determined by the boundary condition. Consider a free liquid surface. In this limit, because of the slip boundary condition, the fluctuating velocity components parallel to the surface, u and v, are nonzero as $z \to 0$ (in contrast to a solid boundary, where the no-slip boundary condition ensures that u and v approaches zero as $z \to 0$). The surface normal component, w, will approach zero as $z \to 0$ because of kinematic blocking, since we assume the surface remains flat and undisturbed in this case. The fluctuating concentration approaches zero as the surface is approached (since the concentration is assumed constant on the surface). Thus, as $z \to 0$: $u \to a_0$, $v \to b_0$, $w \to z$, and $c \to z$. It should be noted that a_0 and b_0 may depend weakly on the horizontal directions since we are considering finite pool sizes. The near-surface limiting behavior (as $z \to 0$) of the wall-normal scalar flux component can thus be written as

$$\langle cw \rangle \propto \alpha_T \propto z^2. \tag{3.8}$$

The dominating physical processes within turbulent boundary layers depend on the physical distance from the boundary. In the near-wall limit, as considered here, it is customary to introduce a scaling proportional to the Kolmogorov (viscous) length scale; $z^+ = z u_* / \nu$, where $\nu \equiv \mu/\rho$ is the kinematic viscosity of the air, μ and ρ are the corresponding molecular viscosity and density, respectively, and u_* is the friction velocity defined as: $u_* \equiv \sqrt{\tau_{surface}/\rho}$, where $\tau_{surface} = \mu (dU/dz)_{z=0}$ is the frictional force on the boundary ($z = 0$). The viscous scale inside a turbulent flow is thus not a geometrical property per se, but depends on the flow field itself; $z^+ = 1$ equals the Kolmogorov scale signifying the smallest turbulent spatial scale, which varies significantly in size with varying Reynolds number.

The viscous scaling applies very near the wall, formally when $z^+ \ll 1$ but in practice within the so-called linear sub-range: $z^+ \leq \mathcal{O}(1)$ [12]. By scaling the eddy diffusivity with the kinematic viscosity, the following expression is found:

$$\frac{\alpha_T}{\nu} \propto \mathcal{A} \frac{z^2}{\nu} \tag{3.9}$$

where $\mathcal{A}$ is a parameter with dimensions [1/s]. The turbulent length and time scales close to the surface are: $l^+ = \nu/u_*$ and $t^+ = \nu/u_*^2$. Then by dimensional arguments, we assume $\mathcal{A}$ takes the form

$$\mathcal{A} = \frac{1}{t^+} = \frac{u_*^2}{\nu}. \tag{3.10}$$

and thus

$$\alpha_T = \frac{u_*^2 z^2}{\nu} \tag{3.11}$$

We introduce the following non-dimensional variables: $\alpha_T^* = \alpha_T/\nu = z^{+2}$, $\alpha^* = \alpha/\nu = Sc^{-1}$, $C^* = C/C_{ref}$, $z^+ = zu_*/\nu$, and $t^* = tu_*^2/\nu$, where $Sc = \nu/\alpha$ is the Schmidt number and C_{ref} is taken as the saturation concentration: $C_{ref} = C_0$. With this, (3.7) can be rewritten as

$$\frac{\partial C^*(z,t)}{\partial t^*} = \left(Sc^{-1} + z^{+2}\right)\frac{\partial^2 C^*(z,t)}{\partial z^{+2}} + \frac{\nu \mathcal{S}(\mathbf{x},t)}{C_{ref}u_*^2}. \tag{3.12}$$

By using (3.5) this can be written as

$$\delta_m^{-1}\frac{\partial C^*(z,t)}{\partial t^*} = \left(Sc^{-1} + z^{+2}\right)\frac{\partial^2 C^*(z,t)}{\partial z^{+2}} \approx z^{+2}\frac{\partial^2 C^*(z,t)}{\partial z^{+2}} \tag{3.13}$$

Here we have assumed that $z^{+2} \gg Sc^{-1}$ which physically is equivalent to the assumption that turbulence mixing dominates the convective evaporation. It should be noted that although the viscous stresses dominate in the near-surface limit, the turbulence still plays an important indirect role also here, and can not therefore simply be neglected.

We will consider two different models for the *a priori* unknown vapor velocity in equation 3.6: The first assumes that the vapor velocity equals the mean streamwise velocity in the linear sub-layer, $v_{vapor} = K_1 u_*^2/\nu$, where K_1 is a model coefficient (model A); the second model takes v_{vapor} to be equal the friction velocity, $v_{vapor} = u_*$ (model B). For model A, the area in equation 3.6 is then taken as $A_{0,A} = 2rK_1$, where K_1 is related to the thickness of the linear sub-layer and r is the horizontally projected radius of the droplet. For model B the area is taken to be the horizontally projected area of the liquid pool or droplet, $A_{0,B} = \pi r^2$. We assume a constant area for both models and that the droplets are fixed to the boundary without any motion in the streamwise direction. The integral (3.6), can then be rewritten as $\int\int\int C dt dA = A_0 \int_0^t C dt$. The first model is appropriate for small liquid droplets, where the advective time scale for the transportation in the stream wise direction is much less than the evaporation time scale. For larger liquid surfaces, model B might be more appropriate.

We thus have

$$\delta_m^A = \frac{u_* A_{0,A}\int C(\mathbf{x},t)dt}{m_0} \approx \frac{K_1 C_0 A_{0,A} t^*}{2m_0} \tag{3.14}$$

and

$$\delta_m^B \approx \frac{C_0 A_{0,B}\nu t^*}{2u_* m_0} \tag{3.15}$$

where we have approximated the integral by the simple formula $\int C(\mathbf{x},t)dt \approx C_0 t/2$, where C_0 is the saturation concentration. We thus have:

$$\frac{\beta^{A,B}}{t^*}\frac{\partial C^*(z,t)}{\partial t^*} = z^{+2}\frac{\partial^2 C^*(z,t)}{\partial z^{+2}} \tag{3.16}$$

where

$$Model\ A: \quad \beta^A = \frac{2m_0}{K_1 C_0 A_{0,A}}. \tag{3.17}$$

and

$$Model\ B: \quad \beta^B = \frac{2m_0 u_*}{C_0 A_{0,B}\nu}. \tag{3.18}$$

3.2 Algebraic evaporation models

In this section we seek an algebraic solution to (3.16). By separation of variables: $C(z^+,t^*) = \mathcal{T}(t^*)\mathcal{Z}(z^+)$, (3.16) can be rewritten as:

$$\underbrace{\frac{\beta^{A,B}}{\mathcal{T}(t^*)t^*}\frac{d\mathcal{T}(t^*)}{dt^*}}_{=-\lambda} = \underbrace{\frac{z^{+2}}{\mathcal{Z}(z^+)}\frac{d^2\mathcal{Z}(z^+)}{dz^{+2}}}_{=-\lambda} \tag{3.19}$$

The solution to these equations are obtained by recognizing that both sides must be equal to a constant, say $-\lambda$. Thus we have a set of ordinary differential equations that easily can be solved analytically.

The left hand side reads

$$\frac{d\mathcal{T}(t^*)}{\mathcal{T}} = -\left(\lambda/\beta^{A,B}\right)t^* \tag{3.20}$$

which has the solution

$$\mathcal{T}^{\mathcal{A},\mathcal{B}}(t^*) = \mathcal{B}\,exp\left(-\frac{\lambda}{2\beta^{A,B}}t^{*2}\right) \tag{3.21}$$

where $\mathcal{B}$ is a constant. The corresponding equations for the right hand side of (3.19) reads

$$\frac{z^{+2}}{\mathcal{Z}(z^+)}\frac{d^2\mathcal{Z}(z^+)}{dz^{+2}} = -\lambda. \tag{3.22}$$

and has the solution

$$\mathcal{Z}(z^+) = \sqrt{z^+}\left(\mathcal{C}z^{+\gamma} + \frac{\mathcal{D}}{z^{+\gamma}}\right) \tag{3.23}$$

where $\gamma = \frac{1}{2}\sqrt{(1-4\lambda/z^{+2})}$, and $\mathcal{C}$, $\mathcal{D}$, and λ are constants. The validity of the solution thus depends on the liquid-air frictional forces; $4\lambda < z^{+2}$. However, since λ is a constant, and not allowed to explicitly depend on z^+, the applicability of the model varies and there is need to be check this from case to case. This constraint is however not expected to pose a severe limitation to the applicability of the model. Recall that the present analysis is based on the near-surface asymptotics formally valid only for $z^+ \ll 1$; in practice $z^+ \leq \mathcal{O}(1)$ suffice [12]. Here we will use $\lambda/z^+ \ll 1$ so $\gamma \approx 1/2$; the solution (3.23) thus simplifies to $\mathcal{Z}(z^+) \approx \mathcal{C}z^+$.

The non-dimensional solutions can now be written as

$$C^{*A,B}(z^+,t^*) = \mathcal{F}^{A,B}\,z^+ exp\left(-\frac{\lambda}{2\beta^{A,B}}t^{*2}\right) \tag{3.24}$$

where $\mathcal{F}^{A,B}$ are non-dimensional model constants. Recall that $z^+ = zu_*/\nu$ and $t^* = tu_*^2/\nu$. Here z is the physical distance to the liquid-air interphase.

The final solutions can now be written as:

$$C^{A,B}(u_*,t) = C_0\mathcal{G}_{A,B}\frac{u_*}{\nu}\,exp\left(-\mathcal{H}^{A,B}t^2\right). \tag{3.25}$$

where $\mathcal{G}_A$ and $\mathcal{G}_B$ are *a priori* unknown coefficients with dimensions m, and

$$\mathcal{H}^A = \frac{K_1 C_0 \lambda A_{0,A} u_*^4}{4m_0\nu^2}. \tag{3.26}$$

and

$$\mathcal{H}^B = \frac{C_0\lambda A_{0,B}u_*^3}{4m_0\nu}. \tag{3.27}$$

3.2.1 Model for the total evaporation time

The total evaporation time τ_∞ can be estimated by considering the relation

$$m_0 = v_{vapor} A_0 \int_0^{\tau_\infty} C(u_*, t) dt \tag{3.28}$$

Recall that $v_{vapor} = K_1 u_*^2/\nu$ (model A) and $v_{vapor} = u_*$ (model B). Integrating (3.25) gives

$$erf(\sqrt{\mathcal{H}^{A,B}}\tau_\infty) = \mathcal{L} \tag{3.29}$$

where

$$\mathcal{L} = \frac{2m_0\nu\sqrt{\mathcal{H}^{A,B}}}{C_0 \mathcal{G} A_{0,A,B} v_{vapor} u_* \sqrt{\pi}}. \tag{3.30}$$

By approximating the error function in (3.29) as

$$erf(\sqrt{\mathcal{H}^{A,B}}\tau_\infty) \approx \left(1 - exp(-\frac{4\mathcal{H}^{A,B}\tau_\infty^2}{\pi}\right)^{1/2} \tag{3.31}$$

the following estimate of the total evaporation time is found

$$\tau_\infty^{A,B} \approx \sqrt{-\frac{\pi}{4\mathcal{H}^{A,B}} ln\,(1 - \mathcal{L}^2)}. \tag{3.32}$$

3.3 Odd Busmundrud's model

As previously mentioned, Odd Busmundrud developed a model for evaporation from surfaces or droplets [10]. In this model, evaporated mass is assumed to be transported by molecular diffusion through a still diffusion layer above the surface. Vapor outside this diffusion layer is assumed to be carried away by the wind field. Based on this he derived the following equation for the evaporation rate J

$$J = \alpha \frac{C_0(T)}{\delta} A \tag{3.33}$$

where α is the molecular diffusion coefficient, C_0 the saturation concentration, and δ is the thickness of the diffusion layer. It is assumed that the concentration immediately above the surface equals the saturation concentration and that the concentration at $z = \delta$ is zero. The diffusion layer thickness is calculated from the mean streamwise wind velocity by the empirical relation

$$\delta = 1.6 \cdot 10^{-3} U^{-0.7}. \tag{3.34}$$

An equation for the diffusion coefficient (in m^2/s) of vapor A through a gas B is found in [13]

$$\alpha_{AB} = \frac{4.14 \cdot 10^{-4} T^{1.9} \sqrt{1/MW_A + 1/MW_B}(MW_A^{-0.33}}{p}, \tag{3.35}$$

where MW_A and MW_B are the molecular weights for vapor A and gas B (in g/mol) and p the air pressure (in Pa). Odd Busmundrud's model is in the following labeled model C.

V (μl)	T (°C)	u$_*$ (m/s) (Estimated)	$\tau_{\infty,A}$ (hours)	$\tau_{\infty,B}$ (hours)	$\tau_{\infty,C}$ (hours)	$\tau_{\infty,exp}$ (hours) (Estimated)
1	15	0.14	10.5	9	23.5	9-10
1	15	0.18	6.5	6	14	7-8
1	35	0.09	5.5	4	15	4-5
1	35	0.14	2.5	2	4	2
6	15	0.14	19.5	12	42.5	20-24
6	35	0.09	10	5	27.5	14-15
6	35	0.14	4	2.5	7	4.5-5
6	35	0.17	3	2	5	3.5-4
9	15	0.17	15	9.5	33.5	20
9	35	0.14	5	3	8	4

Table 4.1 Total evaporation times calculated with models A, B and C, and estimated from the experimental data [9] as a function of friction velocity and free-stream temperature.

4 Results

The value of the free parameter $\mathcal{G}$ is calculated from equation 3.29 using the fact that the error function approaches a value of one when $t = \tau_\infty$. This leads to the expression

$$\mathcal{G} = \frac{1}{K_2} \frac{2m_0\nu\sqrt{\mathcal{H}^{A,B}}}{C_0 v_{vap} u_* A_{0,A,B}\sqrt{\pi}} \tag{4.1}$$

where the dimensionless parameter K_2 is taken close but not equal to unity (cf. equations 3.29 and 3.32). There are three free parameters for model A: λ, K_1 and K_2, and two free parameters for model B: λ and K_2. K_1 and K_2 were set equal to $4 \cdot 10^{-4}$ and 0.9 respectively, while $\lambda = 1.5 \cdot 10^{-8}$ at $T = 15$°C and $\lambda = 6 \cdot 10^{-8}$ at $T = 35$°C. The values of λ are chosen by curve fitting to one single data set for each of the temperature. These two values were then kept constant for all the remaining data sets. The values for K_1 and K_2 are kept constant for all sets.

The predicted total evaporation time (3.32) compared with the experimental data are given in table 4.1. Figure 4.1 shows the variation of the remaining mass fraction and the evaporation rate as a function of time. The following cases are displayed: two datasets with temperature $T = 15$°C and initial volume $V = 1\mu$l and two datasets with temperature $T = 35$°C and volume $V = 1\mu$l. Figure 4.2 shows the corresponding results for two datasets for droplets of initial size $V = 6\mu$l and a temperature $T = 35$°C, and two data sets for droplets with an initial volume of $V = 9\mu$l and $T = 15$ and 35°C.

The functional form of the evaporation rate curves are fairly well reproduced by both models. Model A gives reasonably good agreement with the experimental data, which is consistent with the predicted total evaporation times in table 4.1. While model B gives a good agreement with two data sets in figure 4.1, there are a few cases where the model differs substantially from the experimental results, notably in figure 4.2 where the evaporation rate, and the time for the evaporation, is overpredicted by about a factor of three for small values of u_*. Also a few other cases (see table 4.1) shows

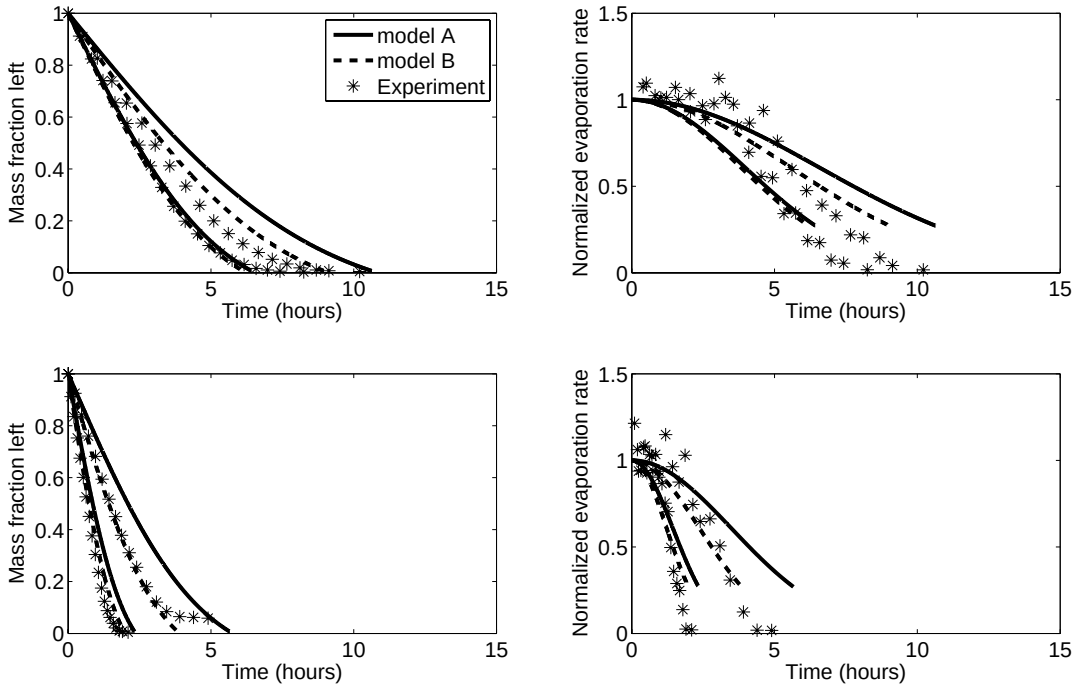

Figure 4.1 Mass fraction of liquid remaining (left) and the normalized evaporation rate (right) as function of time for droplets of $V = 1\mu l$ and $T = 15°C$ (top) and 35 °C (bottom). The data are for $u_* = 0.18$ m/s ($U_\infty = 3.66$ m/s and T.I. 2.8 %) (top and bottom), 0.14 m/s ($U_\infty = 1.77$ m/s and T.I. 2.2 %) (top) and 0.09 m/s ($U_\infty = 0.26$ m/s and T.I. 1.5 %) (bottom).

similar disagreement. This supports the hypothesis that the mean stream wise velocity in the linear sub-layer is the appropriate velocity scale for the transport of vapor from such a small surface. It can thus be concluded that model A is the most suitable choice to estimate the effect of the friction velocity on the rate of evaporation.

Figure 4.3 shows the predicted effect of the friction velocity on the evaporation rate using model A for a range of u_*; the temperature is 15 °C and the initial volume of the droplets are 1 μl.

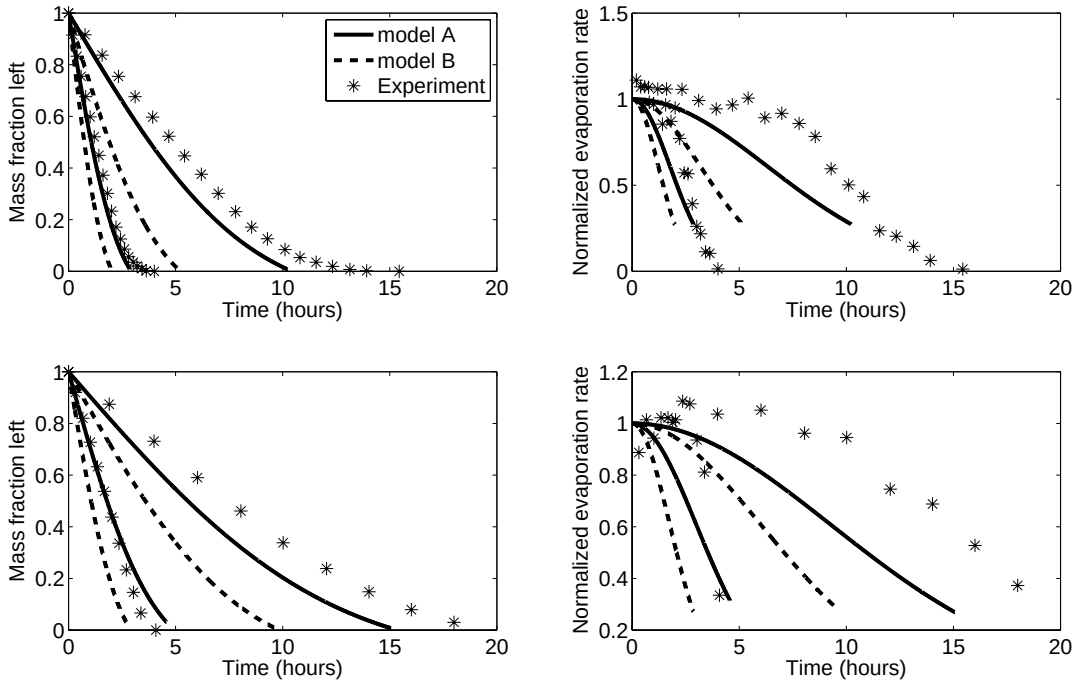

Figure 4.2 Mass fraction of liquid remaining (left) and the normalized evaporation rate (right) as function of time for droplets of $V = 6\mu l$ and $T = 35°C$ (top) and for droplets with $V = 9\mu l$ and $T = 15$ and $T = 35°C$ (bottom). In the top figures $u_* = 0.185$ m/s ($U_\infty = 3.66$ m/s and T.I. 2.8 %), and $u_* = 0.09$ m/s ($U_\infty 0.26$ m/s and T.I. 1.5 %), and in the bottom figure u_* = 0.14 m/s ($U_\infty = 1.77$ m/s and T.I. 2.2 %.) and $u_* = 0.17$ m/s ($U_\infty = 3.0$ m/s and T.I. 2.5 %).

5 Concluding remarks

An algebraic evaporation model sensitized to boundary layer turbulence has been developed. Two models for the transport of vapor from the liquid surface were considered; model A takes the vertical vapor velocity to be the mean streamwise velocity in the linear sub-layer whereas model B takes the vertical vapor velocity to be equal the friction velocity. The two models were validated against recent data from wind tunnel experiments of the evaporation of HD [8, 9]. Model A showed generally good agreement with the experiments, while model B showed a fair agreement, at least for large friction velocities, but with substantial deviation for lower friction velocities. This indicates that the mean stream wise velocity in the linear sub-layer is the appropriate velocity scale for the transport of vapor from the liquid surface.

The present models only indirectly accounts for the temperature effects through the variation of material properties. The results showed, however, that the model should be made explicitly dependent of the free stream temperature. This will be considered in future studies. Another leading order effect that also should be considered in future studies in the impacts of stratification caused by the

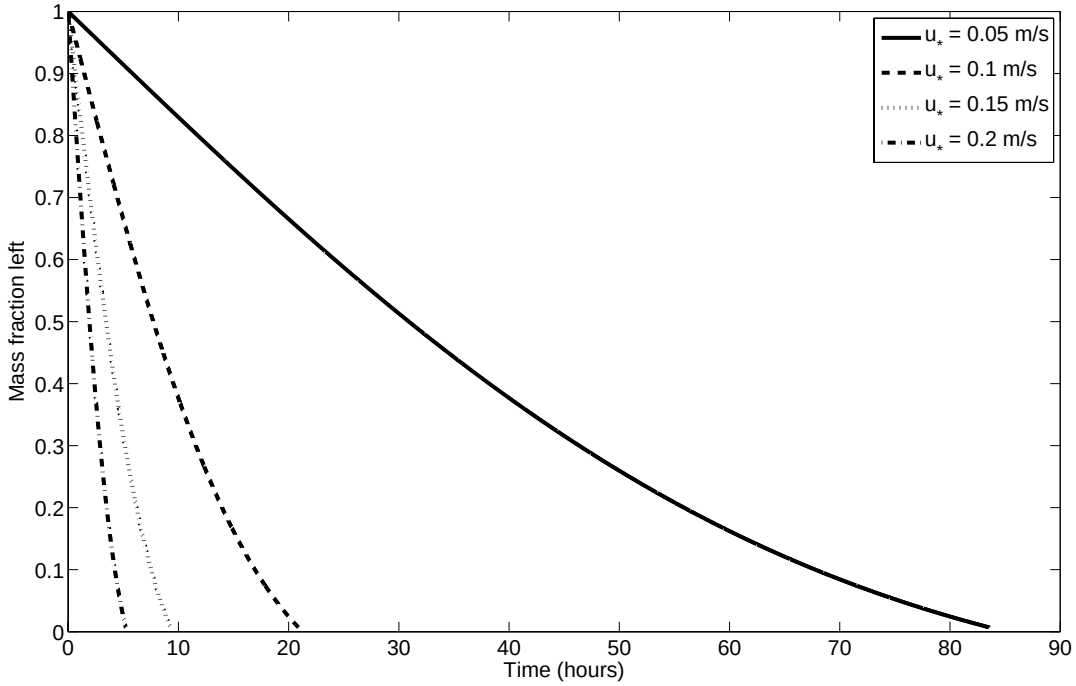

Figure 4.3 The effect of the friction velocity on the evaporation rate calculated with model A. The droplets have a initial volume of 1 μl and the temperature is 15°C.

density difference between the vapor and the air [11]. These aspects were, however, outside the scope of this study.

In this study we have derived a model which is sensitized to the frictional forces acting on the liquid-air interphase. The functional dependence on the friction velocity was analytically derived from the transport equations governing the ensemble averaged concentration field. To the knowledge of the authors, this is the first study of this kind. No *a priori* assumptions about the existence of an equilibrium boundary layer has been made, which increases the applicability of the present model to a wider range of external flow conditions.

There are some uncertainties associated with the data used to validate the models in this study. Firstly, the data are taken directly from [9] by digitizing the plots; it was not possible to get the actual experimental readings. Secondly, [9] does not include estimates of the uncertainties associated with the measurements. In addition, the value of the friction velocity used in the calculations are estimated from other wind speeds and turbulence intensities; to have measurements of the friction velocity at the exact conditions for the evaporation measurements would be highly desirable. Data on the evaporation of toxic chemicals are difficult to find, and a lot of the existing experimental data is sparsely documented with the respect to the fluid dynamical characteristics of the experiment. More experimental data for which the different aspect which influences evaporation (temperature, wind speed, the size of the droplet etc) are systematically varied, is needed. To be able to conduct such measurements ourselves would be very useful.

This work will be continued by including the models in Computational Fluid Dynamics (CFD) software. The models will subsequently be used in dispersion modeling on a local scale (1-2 km^2). It is also an aim to address temperature effects and the impacts of stratification.

References

[1] Thor Gjesdal. Oversikt over modeller for spredningsberegning (an overview of models for dispersion modelling). *FFI/NOTAT-2003/00581*, 2003. Norwegian Defence Research Establishment (In Norwegian).

[2] NATO/RTO/SAS-061. Defence against CBRN-attacks in a changing NATO strategic environment. *NATO/Research and Technology Organization (RTO)/System Analysis and Studies (SAS)-061 Technical Report*, 2009. "RESTRICTED".

[3] S Winter, E Karlsson, S Nyholm, A Hin, and A Oeseburg. Models for the evaporation of chemical warfare agents and other tracer chemicals on the ground. A literature review. *FOA-B–97–00203-864–SE*, 1997. Swedish Defence Research Agency (FOI), Department of NBC defence, S-90182 Umeå , Sweden.

[4] O G Sutton. Wind structure and evaporation in a turbulent atmosphere). *Proc. R. Soc. Lond. A.*, 146:701–722, 1934.

[5] F Pasquill. Evaporation from a plane, free liquid surface into a turbulent air stream. *Proc. R. Soc. Lond. A.*, 182:75–95, 1943.

[6] P W M Brighton. Evaporation from a plane liquid surface into a turbulent boundary layer. *J. Fluid Mech.*, 159:323–345, 1985.

[7] J C R Hund and A H Weber. A lagrangian statistical analysis of diffusion from a ground level source in a turbulent boundary layer. *Q. J. R. Met. Soc.*, 105:423–443, 1979.

[8] B Dooley, D Jeon, and M Gharib. Boundary layer experiments and the agent fate program. *Presented at the Chemical and Biological Defence (CBD) Conference, Baltimore, Md, USA*, 2006.

[9] H K Navaz, E Chan, and B Markicevic. Convective evaporation model of sessile droplets in a turbulent flow - comparison with wind tunnel data. *Int. J. Thermal Sciences*, 47:963–971, 2008.

[10] Odd Busmundrud. Fordamping fra overfalter og dråper (evaporation from surfaces and droplets). *FFI/RAPPORT-2005/03538*, 2005. Norwegian Defence Research Establishment (In Norwegian).

[11] G Desoutter, C Habchi, B Cuenot, and T Poinsot. Dns and modeling of the turbulent boundary layer over an evaporating liquid film. *Int. J. Heat and Mass Transf.*, pages 6028–6041, 2009.

[12] Paul A Durbin and B A Pettersson Reif. *Statistical theory and modeling for turbulent flows, 2nd ed.* John Wiley and Sons, Ltd., 2010.

[13] A A Hummel, K O Braun, and M C Fehrenbacher. Evaporation of a liquid in a flowing airstream. *Am. Ind. Hyg. Ass. J.*, 57:519–525, 1996.